CHIN. PHYS. LETT. Vol. 37, No. 1 (2020) 016101

Supersonic Shock Wave with Landau Quantization in a Relativistic Degenerate Plasma *

M. Kr. Deka[1], A. N. Dev[2]**

[1]Department of Applied Sciences, Gauhati University, Guwahati-781014, Assam, India
[2]Center for Applied Mathematics and Computing, Siksha 'O' Anusandhan (Deemed to be University), Bhubaneswar-751030, Odisha, India

(Received 1 August 2019)

A three-dimensional (3D) Burgers' equation adopting perturbative methodology is derived to study the evolution of a shock wave with Landau quantized magnetic field in relativistic quantum plasma. The characteristics of a shock wave in such a plasma under the influence of magnetic quantization, relativistic parameter and degenerate electron density are studied with assistance of steady state solution. The magnetic field has a noteworthy control, especially on the shock wave's amplitude in the lower range of the electron density, whereas the amplitude in the higher range of the electron density reduces remarkably. The rate of increase of shock wave potential is much higher (lower) with a magnetic field in the lower (higher) range of electron density. With the relativistic factor, the shock wave's amplitude increases significantly and the rate of increase is higher (lower) for lower (higher) electron density. The combined effect of the increase of relativistic factor and the magnetic field on the strength of the shock wave, results in the highest value of the wave potential in the lower range of the degenerate electron density.

PACS: 61.72.J–, 61.50.Ah, 71.20.Nr, 71.55.Gs DOI: 10.1088/0256-307X/37/1/016101

The classical and quantum shock like structures have attracted researchers throughout the world thanks to their potential applications in industry and laboratory.[1–11] The dense degenerate plasmas are ubiquitous in different spaces, as well as in the laboratory, and a few investigations regarding stars and nebulas, where such plasma environments are abundant, have been reported.[12–30] For example, Misra and Ghosh investigated magneto sonic shock like structures in a dissipative quantum plasma considering spin alignment and quantum tunnelling effect, and concluded that both stationary and oscillatory shock structures are possible in such quantum plasma environments.[31–33] In a recent report, Atteya *et al.* investigated shock structures with heavy elements in relativistic quantum plasmas and found that in the presence of low electron density in the ultra-relativistic regime, monotonic shock structures are possible whereas the shock wave amplitude decreases when the density of heavy elements increases.[34] In the same report, they also confirmed that in non-relativistic and ultra-relativistic cases, the solitonic hump decreases with increasing the degenerate Bohm potential. Elliason and Shukla reported the formation of shock waves with degenerate relativistic electrons and concluded that the phase speed of the nonlinear waves increases with increasing the amplitude of the nonlinear waves and shocks.[35] Sahu and Misra observed magnetohydrodynamic shock structures in quantum plasmas with the effect of exchange co-relation and found that instead of pressure gradient and other quantum forces, the exchange correlation force is always dominant and the shock wave can switch from monotonic to oscillatory type in the presence of viscosity effect and/or diffusivity.[36] Hossen and Mamun, in an interesting report, studied the coexistence of solitary and shock structures in a cryogenic quantum plasma and concluded that apart from modifying the basic characteristics of solitary/shock structures, the dissipation effect which results in degenerate ion acoustic shock wave arises due to the strong correlation of cold ions.[37] Zobare *et al.* studied the formation shock wave in degenerate dense plasmas and found that shock wave potential increases significantly when electrons are considered to be ultra-relativistic while ions are non-relativistically degenerate.[38] Akbari–Moghanjoughi investigated the properties of degenerate shock waves in a positive/negative ion plasma and concluded that both compressive as well as rarefactive shock waves can propagate in such a plasma.[39] Dip *et al.* studied the existence of nonplanar solitary and shock waves with the effects of Bohm potentials and Fermi temperatures in a strongly coupled degenerate state and found that the height of the solitary (shock) wave decreases (increases) with increasing the equilibrium electron (positive ion) number density.[40] Roy *et al.* observed either oscillatory or monotonic shock wave structure depending on electron-to-ion density ratio, ion kinematic viscosity and quantum diffraction parameter for ion acoustic solitary/shock waves in an electron-positron-ion plasma.[41] On the other hand, the concept of Landau quantization in strong magnetic field is very important as it can significantly modify the equation of state of electrons by effecting the number of electrons in each discrete level. A few investigations on the propagation large/small amplitude solitary waves with Landau quantized magnetic

*Supported by Manoj Kumar Deka from DST-SERB of India under Grant No YSS/2015/001896.
**Corresponding author. Email: apulnarayandev@soa.ac.in
© 2020 Chinese Physical Society and IOP Publishing Ltd

field have been reported, in which the effect of a high magnetic field on amplitude/width of a solitary wave in the relativistic/non-relativistic plasma regime was studied.[42–45] In this Letter, we discuss the features of shock waves in a relativistic plasma in the presence of Landau quantization, which is important from viewpoints of space and astrophysical plasmas.

The proposed degenerate plasma is composed of cold ions with a magnetically trapped relativistic quantum dense electron fluid. The continuity, momentum and Poisson's equations are as follows:

$$\frac{\partial n_{\rm i}}{\partial t}+\nabla\cdot(n_{\rm i}\boldsymbol{v}_{\rm i})=0 \tag{1}$$

$$\left(\frac{\partial}{\partial t}+\boldsymbol{v}_{\rm i}\cdot\nabla\right)(\gamma_{\rm i}\boldsymbol{v}_{\rm i})=-\frac{Z_{\rm i}q_{\rm i}}{m_{\rm i}}\nabla\phi-\frac{\nabla p_{\rm i}}{m_{\rm i}n_{\rm i}}-\frac{1}{c}\boldsymbol{v}_{\rm i}\times B_0+\mu_{\rm i}\nabla^2 v_{\rm i}, \tag{2}$$

$$\nabla E=4\pi e\left(n_{\rm e}-Z_{\rm i}n_{\rm i}\right), \tag{3}$$

where $E=-\nabla\phi$ with ϕ being the electrostatic potential; $n_{\rm i}$, $n_{\rm e}$, $m_{\rm i}$, $v_{\rm i}$, $q_{\rm i}$ denote the ion density, electron density, mass, velocity, positive ion charge, respectively, and $Z_{\rm i}$ is the charged state of the positive ions. The relativistic factor is $\gamma_{\rm i}=\{1-(v_{\rm i}/c)^2\}^{-1/2}=1+(v_{\rm i}/\sqrt{2}c)^2$ with c being the velocity of light. We have adopted the techniques similar to that taken by Tsintsadze *et al.*[46] for Landau quantized magnetic field and found the normalized electron density as

$$N_{\rm e}=\frac{n_{\rm e}}{n_{\rm e0}}=\frac{3}{2}\frac{1}{\varepsilon_{\rm R}^3}\left\{\left(\eta\varepsilon_{\rm R}^2\sqrt{1-\varepsilon_{\rm R}^2}+\frac{3}{2}(1-\varepsilon_{\rm R}^2-\eta\varepsilon_{\rm R}^2)^{\frac{3}{2}}\right)+\left(\frac{\eta\varepsilon_{\rm R}^2}{\sqrt{1-\varepsilon_{\rm R}^2}}+\frac{9}{2}\sqrt{1-\varepsilon_{\rm R}^2-\eta\varepsilon_{\rm R}^2}\right)\phi+\left(\frac{\eta\varepsilon_{\rm R}^4}{2\sqrt{1-\varepsilon_{\rm R}^2}(\varepsilon_{\rm R}^2-1)}+\frac{9}{4}\frac{\sqrt{1-\varepsilon_{\rm R}^2-\eta\varepsilon_{\rm R}^2}(-2+\varepsilon_{\rm R}^2+\eta\varepsilon_{\rm R}^2)}{(-1+\varepsilon_{\rm R}^2+\eta\varepsilon_{\rm R}^2)}\right)\phi^2\right\}, \tag{4}$$

where $\eta=2\hbar\omega_{\rm ce}/m_{\rm e}c^4$ showing the effect of Landau diamagnetism, $\hbar=h/2\pi$ with h being Planck's constant, $\omega_{\rm ce}=eB_0/m_{\rm e}c$ is the cyclotron frequency with e being the electron charge, $m_{\rm e}$ is the mass of electron, B_0 is the magnetic field, $n_{\rm e0}=p_{\rm F}^3/3\pi^2\hbar^3$ is the equilibrium electron density with $p_{\rm F}$ being the momentum of the Fermi surface, and $\varepsilon_{\rm F}=\left(\hbar^2/2m_{\rm e}\right)\left(3\pi^2 n_{\rm e0}\right)^{2/3}$ is the Fermi energy. Also $\varepsilon_{\rm R}=m_{\rm e}c^2/\mu_{\rm e}$ is the ratio of relativistic electron's rest mass energy to the overall chemical potential, where $\mu_{\rm e}=\varepsilon_{\rm F}+m_{\rm e}c^2$ is the sum of the Fermi energy and the rest mass energy. For positive ions, the adiabatic equation of state is given by $p_j/p_{j0}=(n_{\rm p}/n_{\rm p0})^{\upsilon}=N_{\rm p}^{\upsilon}$, where $p_{i0}=n_{i0}k_{\rm B}T_{\rm i}$, and $\upsilon=(2+N)/N=5/3$ (with N being the number of degrees of freedom) is the adiabatic index for three-dimensional geometry of the system. The normalized set of equations from basic Eqs. (1)–(3) can be written as follows:

$$\frac{\partial N_{\rm i}}{\partial T}+\nabla\left(N_{\rm i}V_{\rm i}\right)=0, \tag{5}$$

$$\frac{\partial\left(\gamma_{\rm i}V_{\rm i}\right)}{\partial T}+V_{\rm i}\nabla\left(\gamma_{\rm i}V_{\rm i}\right)=-\nabla\phi-\frac{5\sigma_{\rm i}\nabla N_{\rm i}}{3N_{\rm i}^{1/3}}-V_{\rm i}\times\Omega_{\rm i}+\rho\nabla^2\left(V_{\rm i}\right), \tag{6}$$

$$\nabla^2\phi=\mu_{\rm e}N_{\rm e}-N_{\rm i}, \tag{7}$$

where $N_{\rm i}$ and $V_{\rm i}$ denote the normalized ion density and ion velocity, respectively. $N_{\rm i}$ is normalized by the equilibrium value n_{i0} and $V_{\rm i}$ by $C_{\rm i}\left(k_{\rm B}T_{\rm i}/m_{\rm i}\right)^{1/2}$; ϕ is the wave potential normalized by $k_{\rm B}T_{\rm i}\phi/e$, the time variable T is normalized by $\omega_{\rm pi}=\left(4\pi n_{i0}e^2/m_{\rm i}\right)^{1/2}$, the space variables are normalized by $C_{\rm i}/\omega_{\rm pi}$ to give us $\omega_{\rm pi}\lambda_{\rm D}=c_{\rm i}$, together with $\rho=\mu_{\rm i}/\omega_{\rm pi}\lambda_{\rm D}^2$, which is the kinematic viscosity where the Debye length $\lambda_{\rm D}=\left(k_{\rm B}T/4\pi n_{i0}e^2\right)^{1/2}$. Here $\mu_{\rm e}=n_{\rm e0}/n_{i0}$, $\sigma_{\rm i}=T_{\rm i}/T_{\rm e}$ with $T_{\rm i}$ and $T_{\rm e}$ being the temperatures of positive ions and electrons, respectively, and $\Omega_{\rm i}=eB_0/m_{\rm i}\omega_{\rm pi}$ is defined as the ion gyro-frequency.

To this set of normalized Eqs. (5)–(7), we introduce the following stretched co-ordinates to derive the 3D Burgers' equation,

$$\xi=\varepsilon\left(X-\lambda T\right),\quad \eta=\varepsilon Y,\quad \tau=\varepsilon^2 T,\quad \rho=\varepsilon^{\frac{1}{2}}\rho_0, \tag{8}$$

where λ is the normalized phase velocity. The dependent variables $N_{\rm i}$, $V_{\rm i}$ and ϕ etc. are expanded in the power series of ε as

$$N_{\rm i}=1+\sum_{j=1}^{\infty}\varepsilon^j N_{\rm i}^{(j)},\quad \phi=\sum_{j=1}^{\infty}\varepsilon^j\phi^{(j)},\quad V_{ix}=V_{i0}+\sum_{j=1}^{\infty}\varepsilon^j N_{\rm i}^{(j)},\quad V_{{\rm i}y,z}=\sum_{j=3/2,k=1}^{\infty}\varepsilon^j V_{{\rm i}y,z}^{(k)}. \tag{9}$$

Substituting Eqs. (8) and (9) into Eqs. (5)–(7), we can model the first order equation as

$$N_{\rm p}^{(1)}=a\,\phi^{(1)},\quad V_{\rm p}^{(1)}=wa\,\phi^{(1)},\quad w=\lambda-{\rm V}_0,\quad a=\left(w^2\gamma_1-5\sigma_{\rm i}/3\right)^{-1}, \tag{10}$$

$$\lambda=\frac{\gamma_1{\rm V}_0\pm\sqrt{\gamma_1^2{\rm V}_0^2+\gamma_1 p}}{\gamma_1}, \tag{11}$$

where $\gamma_1=\left(1+1.5\gamma^2\right)$, $\gamma={\rm V}_0/c$, $p=5\sigma_{\rm i}/3+(\alpha_1\mu_{\rm e})^{-1}-\gamma_1{\rm V}_0^2$.

Similarly, the second order equations, by equating the coefficients of ε^2 from the x, y and z components of Eqs. (5)–(7), are modelled as

$$\frac{\partial N_{\rm i}^{(1)}}{\partial\tau}-w\frac{\partial N_{\rm i}^{(2)}}{\partial\xi}+\frac{\partial V_{ix}^{(2)}}{\partial\xi}+\frac{\partial\left(N_{\rm i}^{(1)}V_{ix}^{(1)}\right)}{\partial\xi}+\frac{\partial V_{iy}^{(1)}}{\partial\eta}+\frac{\partial V_{iz}^{(1)}}{\partial\zeta}=0, \tag{12}$$

$$\gamma_1\frac{\partial V_{ix}^{(1)}}{\partial\tau}-w\gamma_2\frac{\partial V_{ix}^{(1)^2}}{\partial\xi}-w\gamma_1\frac{\partial V_{ix}^{(2)}}{\partial\xi}+\gamma_1 V_{ix}^{(1)}\frac{\partial V_{ix}^{(1)}}{\partial\xi}-\frac{w}{3}\gamma_1 N_{\rm i}^{(1)}\frac{\partial V_{ix}^{(1)}}{\partial\xi}+\frac{\partial\phi^{(2)}}{\partial\xi}+\frac{1}{3}N_{\rm i}^{(1)}\frac{\partial\phi^{(1)}}{\partial\xi}+\frac{5}{3}\sigma_{\rm i}\frac{\partial N_{\rm i}^{(2)}}{\partial\xi}-\rho_0\frac{\partial^2 V_{ix}^{(1)}}{\partial\xi^2}=0, \tag{13}$$

$$\frac{\partial}{\partial\xi}\left(\frac{\partial V_{iy}}{\partial\eta}\right)+\frac{\partial}{\partial\xi}\left(\frac{\partial V_{iz}}{\partial\zeta}\right)=\frac{1}{w}\left(1+\frac{5}{3}\sigma_{\rm i}a\right)\left\{\frac{\partial^2\phi}{\partial\zeta^2}+\frac{\partial^2\phi}{\partial\eta^2}\right\}, \tag{14}$$

$$\frac{\partial N_{\rm i}^{(2)}}{\partial\xi}=\alpha_1\mu_{\rm e}\frac{\partial\phi^{(2)}}{\partial\xi}+2\mu_{\rm e}\alpha_2\phi^{(1)}\frac{\partial\phi^{(1)}}{\partial\xi}, \tag{15}$$

where

$$\alpha_1=\frac{3}{2}\eta\frac{1}{\varepsilon_{\rm R}^3}\left\{\frac{\varepsilon_{\rm R}^2}{\sqrt{1-\varepsilon_{\rm R}^2}}+\frac{9}{2\eta}\sqrt{1-\varepsilon_{\rm R}^2-\eta\varepsilon_{\rm R}^2}\right\},$$

$$\alpha_2=\frac{3}{2}\eta\frac{1}{\varepsilon_{\rm R}^3}\left\{\frac{\varepsilon_{\rm R}^4}{2\sqrt{1-\varepsilon_{\rm R}^2}\,(\varepsilon_{\rm R}^2-1)}+\frac{9}{4\eta}\frac{\sqrt{1-\varepsilon_{\rm R}^2-\eta\varepsilon_{\rm R}^2}\,(-2+\varepsilon_{\rm R}^2+\eta\varepsilon_{\rm R}^2)}{(-1+\varepsilon_{\rm R}^2+\eta\varepsilon_{\rm R}^2)}\right\}.$$

By performing some mathematical calculations through Eqs. (12)–(15) along with Eqs. (10) and (11), the final 3D Burgers' equation describing the evolution of shock wave is obtained as follows:

$$\frac{\partial}{\partial\xi}\left(\frac{\partial\phi^{(1)}}{\partial\tau}+A\phi^{(1)}\frac{\partial\phi^{(1)}}{\partial\xi}-B\frac{\partial^2\phi^{(1)}}{\partial\xi^2}\right)+C\left(\frac{\partial^2\phi}{\partial\zeta^2}+\frac{\partial^2\phi}{\partial\eta^2}\right)=0 \tag{16}$$

where

$$A=\frac{(8\gamma_1 w^2a^2-w^3a^2\gamma_2 6+a)+(2\mu_{\rm e}\alpha_2)(5\sigma_{\rm i}-3w^2\gamma_1)}{6\gamma_1 wa},$$

$$B=\frac{\rho_0}{2\gamma_1},\quad C=\frac{1}{2w}\left(\frac{1}{a}+\frac{5}{3}\sigma_{\rm i}\right),\quad \gamma_2=\frac{3\gamma}{2c}.$$

The stationary solution to the 3D-Burgers Eq. (16) is

$$\phi^{(1)}=\phi_m\left\{1-\tanh\left(\frac{\chi}{\omega}\right)\right\}, \tag{17}$$

where $\phi_m=\{U\,l-C\,(1-l^2)\}/A\,l^2$ and $\omega=2Bl^3/\{U\,l-C\,(1-l^2)\}$ are the height and thickness of the shock wave, respectively, with l representing the direction cosine and U the velocity. Here A is the nonlinear coefficient, B is the dissipative coefficient, and C is the transverse component arising from the magnetic field.

From the analytical solution governed by Eq. (17), we analyze the nature and characteristics of solitary wave propagation under different physical situations. Here we have considered plasma density as 10^{26}–$10^{29}\,{\rm cm}^{-3}$, ambient magnetic field as 10^9–10^{11} Gauss and we find the Fermi temperature for those plasma parameters in the range of 3.6277×10^7 K.[47–50] Throughout the entire analytical observation, we have considered helium positive ions.

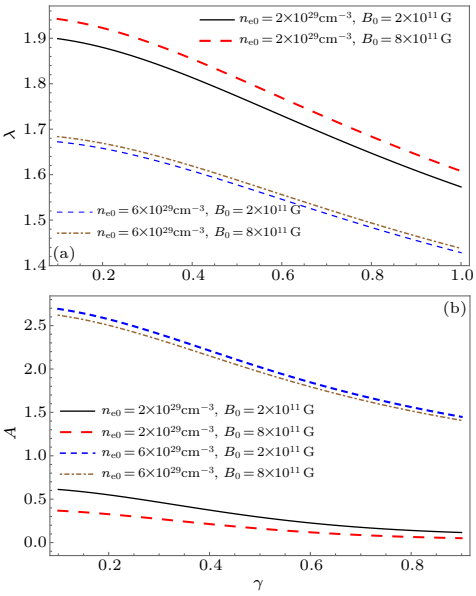

Fig. 1. (a) Variation of normalized phase velocity of the shock wave with relativistic factor γ at different degenerate electron density n_{e0} and magnetic field B_0. (b) Variation of nonlinearity of the plasma system with relativistic factor γ at different degenerate electron density n_{e0} and magnetic field B_0.

Figure 1(a) describes the propagation characteristics of normalized phase velocity with the relativistic factor for different degenerate electron density and quantize magnetic field. On close examination, it can be seen that keeping the electron density fixed, if we increase the magnetic field, the phase velocity will increase (red dashed curves). This may be due to the fact that magnetic field plays the role of confining the plasma species along its direction. Thus, in such a high magnetic field, the plasma particle will move somewhat in a conduit way to reduce the randomized motion and thus may contribute in the enhancement of the average phase velocity. On the other hand, with increasing the degenerate electron density and keeping the quantized magnetic field fixed, the phase velocity decreases (blue dashed curves), significantly compared to the case of similar values of electron density and magnetic field (black solid curves). This is due to the increase in the electron density. Now as seen from Fig. 1, the rate of reduction in the phase velocity with the increasing electron density is much higher than the rate of enhancement in the phase velocity with the increasing magnetic field. This is due to the fact that with such strong magnetic fields, if the electron density is increased, the probable rate of collision will increase significantly due to the channelized propagation of plasma particles along the magnetic field, and the increase in electron density should have a greater impact on the phase velocity compared to the case of increase in magnetic field logically. With increasing electron density, we will have a greater number of

electrons to interact and to collide along a channelized direction due to the presence of magnetic field whereas the increase in magnetic field will force the already available plasma species to move. Another interesting observation from the figure is that the rate of increase of average phase velocity with magnetic field for lower electron density is higher than that for higher electron density, which is obvious from the above discussion. It is also observed that for all the cases discussed above, the phase velocity decreases with increasing relativistic factor γ. Figure 1(b) demonstrates the characteristic variation of A, which is the nonlinear coefficient at different degenerate electron densities and magnetic field strengths. As seen from the figure, with increasing magnetic field, the nonlinearity of the plasma system decreases whereas an enhancement of electron density can increase the value of the nonlinear coefficient of the plasma system for the obvious reason discussed in detail in the case of Fig. 1(a). The rate of reduction of nonlinearity with magnetic field with lower electron density (black solid curves and red dashed curves) is greater than that with higher electron density (blue dashed curves and brown dot-dashed curves). On the other hand, with the relativistic factor, the nonlinearity goes down for all the cases discussed in the figure.

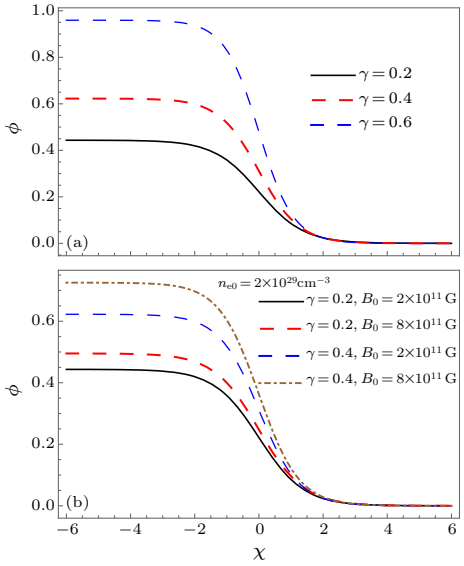

Fig. 2. (a) Variation of the shock wave potential with relativistic factor γ, where the other plasma parameter are considered as $n_{e0} = 2 \times 10^{29}\,\text{cm}^{-3}$ and $B_0 = 2 \times 10^{11}$ G. (b) Variation of the shock wave potential with relativistic factor γ for the magnetic field B_0.

Figure 2(a) describes the propagation of shock wave with the relativistic factor γ. As seen from the graph, the shock amplitude increases with the increasing relativistic factor, and the rate of increase of the amplitude of the shock wave with the relativistic factor is higher. It is clear from the evolution equation of shock wave that the maximum amplitude of shock wave is inversely proportional to the nonlinearity of the plasma. Now as seen from the Fig. 1(b), with the relativistic factor, for any plasma condition, the nonlinearity goes down and hence the shock amplitude increases with increase in the relativistic factor. In Fig. 2(b), we sketch the variation of shock wave amplitude with relativistic factor and magnetic field at a particular electron density. It is seen that the shock wave amplitude increases with increasing both the relativistic factor and magnetic field. This is for obvious reason discussed above. However, the rate of increase of wave amplitude is higher (blue dashed curves and brown dot-dashed curves) when the magnetic field increases at a higher value of relativistic factor. This is because the velocity of the plasma species also increases with increasing relativistic factor, and it is well known that once plasma becomes magnetized, the particles with higher velocity will have a greater tendency of being trapped in the magnetic field and hence a low diffusion rate from the plasma, and they are forced to move in a ductus way reducing the nonlinearity further which allows the shock to propagate with a higher amplitude.

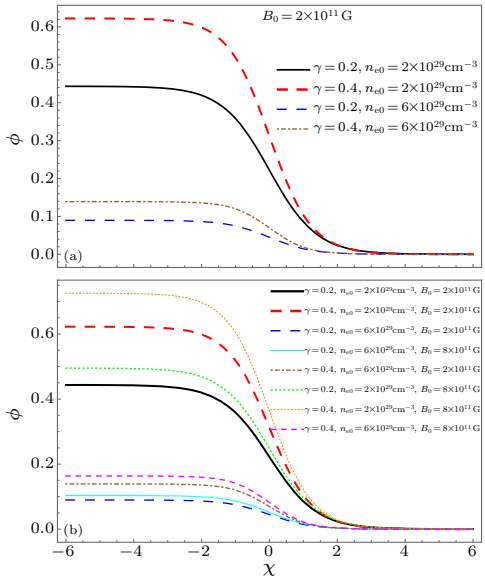

Fig. 3. (a) Variation of the shock wave potential with relativistic factor γ and degenerate electron density n_{e0}. (b) Combined effect of relativistic factor γ, degenerate electron density n_{e0}, and magnetic field B_0, on the shock wave potential.

Figure 3(a) describes the variation of height (amplitude) of the shock wave with relativistic factor and electron density at a particular magnetic field strength. It is seen that the shock wave's amplitude decreases significantly with increasing electron density (black solid curves and blue dashed curves). This is obviously due to the higher rate of increase of nonlinearity of the plasma system with the increasing plasma electron density in the background ambient magnetic field. This happens because the magnetic field will enforce the behavior of the plasma particles in a ductus way. In this situation, if electron density increases, then we can expect a higher rate of probable collision which increases the nonlinearity of the plasma significantly decreasing the phase velocity. Therefore, the shock wave's amplitude decreases significantly. On the other hand, as discussed above the shock wave amplitude increases as the relativistic

factor γ increases, but the rate of increase of shock wave potential is much higher (black solid curves and red dashed curves) when the electron density is low while it is in the much lower side (blue dashed curves and brown dot-dashed curves) when the electron density is high. Reasonably, as γ increases the nonlinearity decreases (Fig. 1(b)) and hence shock potential increases, but as γ increases in the presence of such high background ambient magnetic field, the faster particles are easily available to undergo frequent collision with the increased number of electron density which is not in the case of low electron density (black solid curves and red dashed curves). Thus, the nonlinearity of the plasma system is much higher with higher electron density and faster plasma particles (as γ is higher) and hence shock potential increases with a much lower rate.

In Fig. 3(b), we place a comparative study of the effect of various plasma parameters on the propagation characteristics of supersonic shock waves. As seen from the figure, the amplitude of the shock wave is the highest when the magnetic field and the relativistic factor increase simultaneously (top dotted orange curve) and the amplitude is the lowest when electron density increases with magnetic field and the relativistic factor decreasing simultaneously (blue dashed curve). Reasonably, the faster rate of decrease of nonlinearity with simultaneous increases in the magnetic field and the relativistic factor at low electron density and the faster rate of increases of nonlinearity with simultaneous increases in the magnetic field and the relativistic factor at higher electron density, for the present plasma system, we can know that the maximum of shock wave amplitude is an inverse function of the nonlinearity of the plasma system. On the other hand, the shock wave amplitude always increases with a higher rate when the relativistic factor and magnetic field increase at lower electron density whereas the same increases at very lower rate when the electron density is higher. For example, considering the values of γ, n_{e0} and B_0 adopted for the black solid curve as base values, if γ and B_0 are increased, the shock wave potential increases (red dashed curves and green dotted curve) and this rate of increase is greater with the increase of the relativistic factor. Similar is the physical situation for the bottom curves of the plot. Considering the values of γ, n_{e0} and B_0 adopted for the blue dashed curves as base values, if γ and B_0 are increased, the shock wave potential increases (brown dot-dashed curve and the cyan thin curve) and this rate is very low compared to the low electron density case discussed above. The physics behind all these types of variations can be understood from the detailed discussion placed in the proper context of Figs. 2(a), 2(b) and 3(a) respectively.

In summary, we have found that in a Landau quantized plasma, when the electron density is low, both the relativistic factor and the magnetic field have an incredible effect on the amplitude of the shock wave, whereas for a higher range of electron density, the electron density takes over all the control of the propagation characteristics of shock waves. The rate of increase of shock wave potential with magnetic field and relativistic factor is the highest when the electron density is on a lower side, the same trend is maintained with higher electron density but with a low rate of increase.

References

[1] Akhtar N and Hussain S 2011 *Phys. Plasmas* **18** 072103
[2] Sahu B and Roychoudhury R 2007 *Phys. Plasmas* **14** 072310
[3] Marklund M et al 2005 *Europhys. Lett.* **72** 950
[4] Bychkov V et al 2008 arXiv:0801.1295 [physics.plasm-ph]
[5] Dev A N and Deka M K 2017 *Braz. J. Phys.* **47** 532
[6] Dev A N and Deka M K 2018 *Phys. Plasmas* **25** 072117
[7] Dev A N and Sarma J et al 2015 *Plasma Sci. Technol.* **17** 268
[8] Dev A N et al 2015 *J. Korean Phys. Soc.* **67** 339
[9] Dev A N et al 2014 *Commun. Theor. Phys.* **62** 875
[10] Dev A N et al 2015 *Can. J. Phys.* **93** 1030
[11] Deka M K and Dev A N 2018 *Plasma Phys. Rep.* **441**
[12] Shukla P K and Eliasson B 2006 *Phys. Rev. Lett.* **96** 245001
[13] Brodin G and Marklund M 2007 *Phys. Rev. E* **76** 055403
[14] Brodin G et al 2008 *Phys. Rev. Lett.* **100** 175001
[15] Shukla P K and Eliasson B 2010 *Phys. Usp.* **53** 51
[16] Haas F 2011 *Quantum Plasmas: An Hydrodyanmic Approach* (New York: Springer)
[17] Chandrasekhar S 1931 *Philos. Mag.* **11** 592
[18] Chaichian M et al 2000 *Phys. Rev. Lett.* **84** 5261
[19] Fortov V F 2009 *Phys. Usp.* **52** 615
[20] Glenzer S H et al 2007 *Phys. Rev. Lett.* **98** 065002
[21] Dariescu C and Dariescu M A 2010 *Chin. Phys. Lett.* **27** 011101
[22] Sakalli I and Halilsoy M 2011 *Chin. Phys. Lett.* **28** 070402
[23] Sun X D et al 2014 *Chin. Phys. B* **23** 060401
[24] Goyal N and Gupta R K 2012 *Chin. Phys. B* **21** 090401
[25] Gao Y J 2004 *Chin. Phys. B* **13** 602
[26] Nashed Gamal G L 2011 *Chin. Phys. B* **20** 020402
[27] Sharif M and Yousaf Z 2012 *Chin. Phys. Lett.* **29** 050403
[28] Zhou K et al 2012 *Chin. Phys. B* **21** 020401
[29] Sharif Mamd Azam M 2013 *Chin. Phys. B* **22** 050401
[30] Azam M et al 2016 *Chin. Phys. Lett.* **33** 070401
[31] Misra A P and Ghosh N K 2008 *Phys. Lett. A* **372** 6412
[32] Dev A N 2017 *Chin. Phys. B* **26** 025203
[33] Dev A N et al 2016 *Chin. Phys. B* **25** 105202
[34] Atteya A et al 2017 *Eur. Phys. J. Plus* **132** 109
[35] Eliasson Band Shukla P K 2012 *Europhys. Lett.* **97** 15001
[36] Sahu B and Misra A P 2017 *Eur. Phys. J. Plus* **132** 316
[37] Hossen M A and Mamun A A 2015 *Phys. Plasmas* **22** 073505
[38] Zobaer M S et al 2013 *J. Plasma Phys.* **79** 65
[39] Moghanjoughi M A 2012 *Open J. Acoust.* **2** 72
[40] Dip R D et al 2017 *J. Korean Phys. Soc.* **70** 777
[41] Roy K, Misra A P and Chatterjee P 2008 *Phys. Plasmas* **15** 032310
[42] Irfan M et al 2017 *Phys. Plasmas* **24** 052108
[43] Iqbal M J et al 2017 *Phys. Plasmas* **24** 014503
[44] Shah H A et al 2011 *Phys. Plasmas* **18** 102306
[45] Deka M K and Dev A N 2018 *Ann. Phys.* **395** 45
[46] Tsintsadze N L and Tsintsadze L N 2014 *Eur. Phys. J. D* **68** 117
[47] Koester D and Chanmugam G 1990 *Rep. Prog. Phys.* **53** 837
[48] Landstreet J 1967 *Phys. Rev.* **153** 1372
[49] Lipunov V M 1992 *Astrophysics of Neutron Stars* (Berlin: Springer-Verlag Press)
[50] Ghosh S S and Lakhina G S 2004 *Nonlinear Processes Geophys.* **11** 219